Journal of Molecular Catalysis A: Chemical 296 (2008) 28–35

Contents lists available at ScienceDirect

Journal of Molecular Catalysis A: Chemical

journal homepage: www.elsevier.com/locate/molcata

Microperoxidase-11-NH_2-FSM16 biocatalyst: A heterogeneous enzyme model for peroxidative reactions

B. Mohajerani[a], M. Soleymani-Jamarani[a], K. Nazari[a,*], A. Mahmoudi[b], A.A. Moosavi-Movahedi[b]

[a] Research Institute of Petroleum Industry, P.O. Box 18745/4163, Tehran, Iran
[b] Institute of Biochemistry and Biophysics, University of Tehran, Tehran, Iran

ARTICLE INFO

Article history:
Received 30 May 2008
Received in revised form 15 August 2008
Accepted 30 August 2008
Available online 5 September 2008

Keywords:
Mesoporous silica
Microperoxidase-11
Nanobiocatalyst
Modification
Heterogeneous model enzyme

ABSTRACT

FSM16 mesoporous silicate and its chemically modified samples were synthesized. Then the relevant nanobiocatalysts consisting of Fe(III)protoporphyrin(IX) (Hemin, Fe(III)PPIX), microperoxidase-11 and horseradish peroxidase were obtained via direct immobilization of the biocatalysts in the nanopores of amine modified FSMs. The prepared catalysts were characterized by XRD, ASAP and diffuse reflectance UV/Vis techniques. The performances of the obtained peroxidase model nanostructures were evaluated by some typical test reactions, such as oxidation of ABTS, *ortho*-methoxyphenol (guaiacol) and peroxidatic synthesis of indophenol and *N*-antipyryl-*p*-benzoquinoneimine. Kinetic parameters including initial reaction rates, rate constants, V_{max}, turnover number, Michaelis constant and catalytic efficiency were obtained and compared to those of Fe(III)PPIX/MCM41 (as a blank) and homogeneous native horseradish peroxidase (HRP). Results showed that MP-11-NH_2-FSM16 nanobiocatalyst is able to mimic horseradish peroxidase with a K_m value of $55.45 \pm 1.29\,\mu M$ with respect to ABTS and guaiacol (as the reducing substrates of HRP). The prepared nanobiocatalysts with high catalytic efficiencies about $10^8\ M^{-1}\ min^{-1}$ showed high peroxidatic activity for oxidation and conversion of aromatic substrates.

1. Introduction

The discovery of ordered mesoporous materials (OMMs) prepared by the liquid surfactant templates has been a significant breakthrough in the catalysis by porous materials. OMMs offer unique potential for the immobilization of catalysts and biocatalysts regarding their ordered, homogeneous and large pores. Biocatalysis plays important role in clean production of energy and fuels, fine chemicals, pharmaceuticals, and green processes. Mostly, heterogeneous biocatalysts consist of catalytically active species localized on the surface of a solid support, preferably a porous solid to achieve improved rate, yield and efficiency. In contrast to heterogeneous catalysts, homogeneous ones have disadvantages, such as lower stability and less successful separation from the reaction mixture. The advantages of heterogeneous catalysts over the homogeneous ones are facile separation and recovery, regeneration and reusability of the catalyst and possibility of its using at extreme conditions such as acidic, alkaline and nonaqueous media, higher temperatures and pressures. Green chemistry principles and environmental issues are pushing the new industrial processes towards biotechnological-based industries. Indeed, as the ultimate goal in catalysis science and engineering [1] and in these environmentally conscious and economically pressured days, homogeneous catalysts preferentially need to be replaced by the alternative green solid catalysts. Hence, the selected strategy is immobilization of the homogeneous catalyst on an insoluble support, referred to as *heterogenization of homogeneous catalyst* [2].

Enzymes as the potent biocatalysts with high selectivities, have been used in the food industry for hundreds of years. Currently, enzymes are becoming increasingly important in sustainable technology and green chemistry [3]. The application of an enzyme for a given reaction is often hampered by major limitations such as high cost and low stability. If an enzyme is immobilized on a rigid support, this limitation can be overcome since the immobilized biocatalyst enables easy separation, reusability, and simple operation [4]. Some immobilized enzymes such as glucose isomerase and penicillin G acylase (PGA) have reached large-scale industrial applications [5,6] and immobilization of other enzymes has been of great interest in research [7].

Abbreviations: HRP, horeseradish peroxidase; MP-11, microperoxidase-11; OMMs, ordered mesoporous materials; ABTS, 2,2-azino-di-3-ethyl-benzothiazoline-(6)-sulphonic acid; CTAB, cetyl trimethylammonium bromide; Fe(III)PPIX, iron(III) protoporhyrin IX; Gl, glutaraldehyde; S, aromatic reductant substrate.

* Corresponding author. Tel.: +98 21 44438526; fax: +98 21 55932428.
E-mail address: nazarikh@ripi.ir (K. Nazari).

1381-1169/$ – see front matter © 2008 Elsevier B.V. All rights reserved.
doi:10.1016/j.molcata.2008.08.018

Today, ordered mesoporous materials with uniform pore sizes (2–30 nm); high surface area (~1000 m^2/g) and large pore volume (~1 cm^3/g) are well known [8–10]. Among these materials, FSM16 [8], MCM41 [9], MCM48 [9] and SBA15 [10] have been extensively studied for catalyst immobilization. MCM48 possesses a three-dimensional, bicontinuous cubic pore structure [9]. The availability of ordered mesoporous materials has opened up unprecedented opportunities for immobilizing biocatalysts. The pore size of these ordered materials can be precisely controlled over a wide range and using these solid supports, the heterogeneous single-site catalysis can be achieved [3,11,12]. Over the past ten years, research and development in using mesoporous silicas as carriers for catalysts has advanced rapidly. This topic has been comprehensively reviewed elsewhere [3,11–15].

Depending on the type of the interaction between the catalyst and the solid support, four common methods for the immobilization of homogeneous catalysts can be introduced: covalent binding, electrostatic interaction, adsorption, and encapsulation.

Covalent binding is by far the most frequently used method for immobilization of homogeneous catalysts. Immobilization via electrostatic ionic interactions is conceptually simple, and is a facile method for immobilizing ionic catalysts or those catalysts that can be ionized under the immobilization conditions. While the adsorption method is simple, it tends to yield an unstable catalyst because of the weak interaction between catalyst and support. Encapsulation is the only catalyst immobilization method that does not require any interaction between the catalyst and the support, but the size of the pore-openings in the support must be smaller than the kinetic size of the immobilized catalyst. In addition to these immobilization methods, cross-linking and entrapment of enzymes can also be used [5–7,16–18]. The advantages and disadvantages of the different methods for enzyme immobilization have been discussed elsewhere [19–23]. In general, for efficient immobilization the support can first be functionalized (preferentially). Ordered mesoporous silicas provide excellent opportunities for the immobilization of both homogeneous and enzyme catalysts via covalent binding because of the availability of well-defined silanol groups [24,25]. The major advantage of covalent binding is the stability of the immobilized enzyme, thus minimizing enzyme leaching [26]. Covalent binding of α-L-arabinofuranosidase to an amino-functionalized, bimodal mesoporous silica support revealed that not only the biocatalyst works under a wider range of experimental conditions (lower pH and higher temperatures), but also possesses a higher resistance toward glucose and ethanol in comparison with the free enzyme [27]. Using SBA15 materials with different surface functionalities (–SH, –Ph, –Cl, $–NH_2$, and –COOH) to immobilize trypsin resulted in solving the leaching of the enzyme by using SBA15 functionalized with –SH, –Cl, and –COOH.

It must be noted that the harsh conditions employed during covalent binding can potentially alter the enzyme conformation, thus lowering the enzymatic activity. In addition, binding of the active sites of the enzyme with a support may result in a total loss of the activity. It has been found that PGA physically adsorbed onto the pores of SBA15 silica retains up to 97% of the activity of free PGA, while PGA covalently attached onto the pores of oxirane-grafted SBA15 retains only 60% of the activity [19]. Nevertheless, such a loss in activity can be compensated by the advantages of immobilized enzymes, such as easy separation from the reaction medium, potential reuse, and the possibility of using the immobilized enzyme in a packed-bed or fluidized-bed reactor.

Peroxidase models are capable of catalyzing some peroxidative reactions such as oxidation, epoxidation and hydroxylation of organic compounds [28–30]. Fe(III)protoporphyrin(IX) (Fe(III)PPIX, hemin) as a known catalytic active site finds in hemoproteins like hemoglobin, myoglobin, cytochromes and peroxidases [31,32]. There is great interest in metalloporphyrins for analytical, synthetic and biotechnological purposes. Homogeneous metalloporphyrins and hemoenzymes have low stability in water solutions so that they may become inactivated at extreme conditions (severe acidic or alkaline pHs, high temperatures, high concentrations of peroxide (>2 mM) and in the presence of reactive solvents) [33,34]. The stability of a biocatalyst during synthesis/purification processes and in operational conditions is of vital importance in biotechnology. Several strategies are in hand to increase operational stability of a biocatalyst including the use of stabilizing additives, immobilization, encapsulation, crystallization and media engineering [19,34,35]. Encapsulation of iron(III)protoporphyrin biocatalyst and preparation of a heterogeneous peroxidase model catalyst via direct synthesis of iron(III)protoporphyrin/MCM41 is reported previously [36].

In order to improve the enzyme loading and immobilization, first, FSM16 should be functionalized preferably by using the covalent binding method. The most useful surface functional groups are thiols, carboxylic acids, alkyl chlorides and amines [14]. Other functional groups, such as vinyls, have been found to modify the enzyme's environment by increasing the hydrophobicity of the support surface [37].

Present work discusses a facile procedure for preparation of heterogeneous peroxidase and peroxidase model enzymes along with comparing and characterization of their kinetic behaviour and potential applications for organic synthesis purposes.

2. Experimental

2.1. Materials

Microperoxidase 11 (MP-11, sodium salt), horseradish peroxidase, Fe(III)PPIX (hemin chloride) and cetyl trimethylammonium bromide (CTAB) were obtained from Sigma. Tetramethylammonium hydroxide (TMAOH), hydrogen peroxide, phenol, guaiacol and 2,2-azino-di-3-ethyl-benzothiazoline-(6)-sulphonic acid (ABTS) were purchased from Merck and used without further purification.

Kanemite (a hydrated layer sodium silicate, $NaHSi_2O_5{\cdot}3H_2O$) was prepared from a $NaOH/SiO_2$ mixture (molar ratio 1:1). NaOH was dissolved in a small amount of water, and then the solution was diluted with ethanol so that silica could easily be dispersed result in formation of homogeneous slurry. After evaporation at 50 °C, the resulting paste was dried at 100 °C and finally calcined at 700 °C for 6 h.

All solutions were prepared using deionized water (Barstead NanoPure D4742; E.R. = 18 MΩ).

The obtained molecular sieves were characterized by X-ray diffraction using a Philips-PW model 1840 X-ray diffractometer with Cu Kα radiation.

Furthermore, diffuse reflectance UV/Vis and atomic absorption spectroscopy techniques were used for comparative investigation of various prepared catalysts using Varian Cary 500 and Varian AA200 spectrophotometers, respectively.

2.2. Methods

2.2.1. Synthesis of FSM16 and its modified samples

FSM16 was prepared based on the direct synthesis method as previously reported [38–42]. The silica-surfactant self-assembly process occurs both at the solid–liquid and the liquid–vapor interfaces. Typically, 10.0 g (0.06 mol) kanemite ($NaHSi_2O_5{\cdot}3H_2O$) was dispersed in 100.0 mL of deionised water and then mixed with 100.0 mL 0.2 M CTAB containing 0.5 M triethylbenzene. pH of the solution was adjusted at 9–10 and the mixture was stirred at room

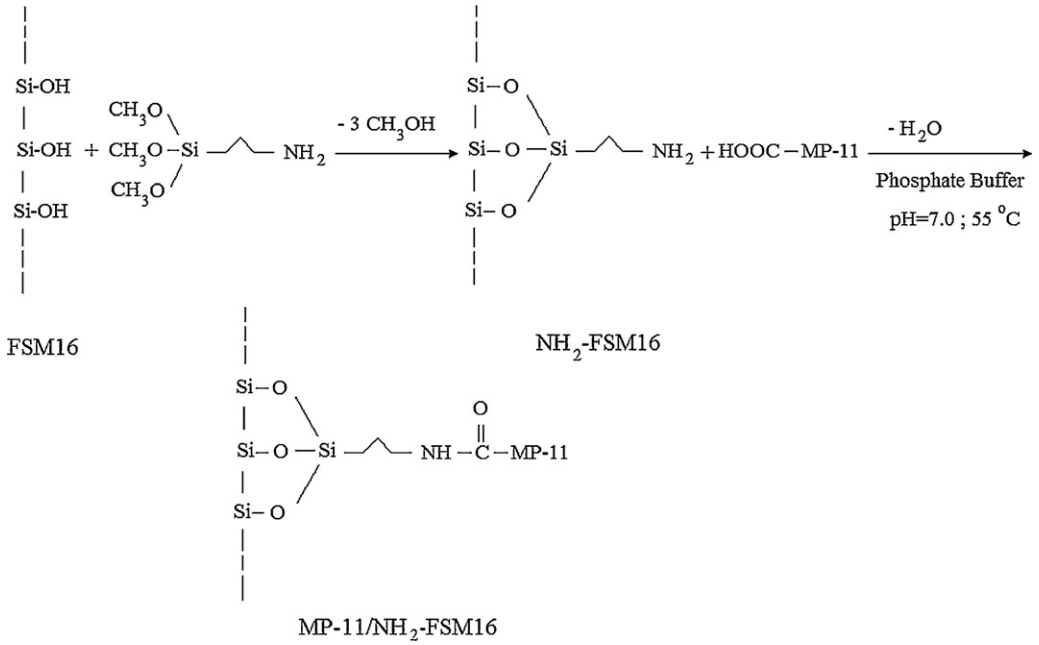

Scheme 1. Typical stepwise modification of FSM16 by 3-aminopropyl trimethoxysilane and preparation of peroxidase model biocatalyst, MP-11-NH_2-FSM16.

temperature for 10 h, and then introduced into a 250 mL volume Teflon stirring reactor at 105 °C to complete the polymerization reaction of silicate [40]. The powdery product was recovered by filtration, and subsequently washed with dilute aqueous HCl–ethanol solution and finally dried in a vacuum oven and then calcined at 500 °C for 1 h. NH_2-FSM16 was prepared by the method, which is reported previously [40]. In summary, 1.00 g FSM16 and 3.99 g 3-aminopropyl trimethoxysilane (0.018 mol) were refluxed under N_2 atmosphere in 30 mL dried toluene at 80 °C for 6 h. Then the product was washed with methylene chloride and diethyl ether (each for 3 times) and dried in a vacuum oven at 70 °C and stored in a vacuum desiccator for the subsequent preparation of biocatalysts. Gl-NH_2-FSM16 was prepared by reacting NH_2-FSM16 with a 5% glutaraldehyde solution (phosphate buffer 5.0 mM, pH 7.0) at room temperature while stirring for about 4 h. The product washed three times with deionized water and dried as described above.

2.2.2. Preparation of biocatalysts

Fe(III)PPIX/NH_2-FSM16 was prepared by direct immobilization of an alkaline solution (pH 8.0) of hemin chloride (15.0 mg, Fe(III)PPIX chloride) into NH_2-FSM16 (200.0 mg) at 55 °C. After efficient washing of the powder (3 times with phosphate buffer solution (5.0 mM, pH 7.0) and 2 times with deionized water) and centrifugation, the obtained biocatalyst was freeze-dried and stored in a vacuum desiccator at 4 °C for further applications. The covalent bonding of Fe(III)PPIX takes place via the preferential reaction of iron atom with the amine group of NH_2-FSM16. The same procedure was used for preparation of MP-11-NH_2-FSM16 (3.0 mg for 200.0 mg FSM16) and HRP-NH_2-FSM16 (5.0 mg HRP for 200.0 mg FSM16) in the phosphate buffer and at 55 °C (far below the thermal transition temperature of HRP, T_m = 85 °C) as shown in Scheme 1. Here, the reaction of amine groups of NH_2-FSM16 with the carboxyl groups of MP-11 and/or HRP amino acid side chains could be introduced as the most probable route for the immobilization process. It must be mentioned that enzyme (hemin, MP-11, HRP) immobilization on the Gl-NH_2-FSM16 did not lead to generation of active heterogeneous peroxidase models probably because of restriction of the pore size of the support (Gl-NH_2-FSM16) as it can be deduced from Fig. 1 (upper pattern). This is the first report on direct immobilization of enzymes on the amine-modified mesoporous materials. The amount of hemin, MP-11 and/or HRP immobilized in NH_2-FSM16 was determined by measuring the iron content of the digested sample in a caustic solution using atomic absorption spectroscopy and were equal to 6.0, 1.2 and 2.0% (w/w), respectively. Regarding the amount of enzymes immobilized, the initial mass of each enzyme and total mass of solid support (200.0 mg), the immobilization yield was obtained 80% for Fe(III)PPIX (12.0/15.0), MP-11 (2.4/3.0) and HRP (4.0/5.0). From the smaller pore size in MCM41 sample and lacking the covalent immobilization for Fe(III)PPIX, it can be seen that loading of hemin into NH_2-FSM16 (6.0%, w/w) was about 7.4 times greater than that for

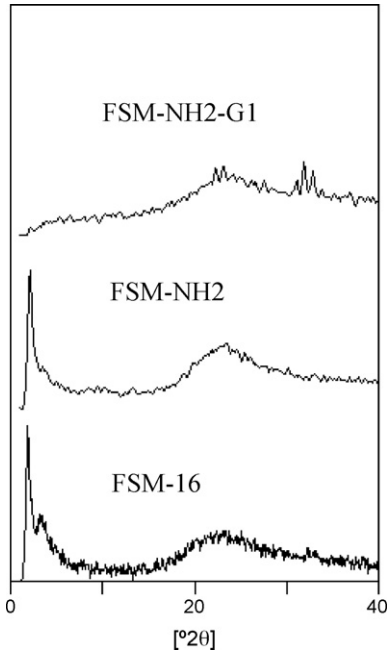

Fig. 1. XRD patterns of the FSM16, NH_2-FSM16 and Gl-NH_2-FSM16.

MCM41 (0.815%, w/w) corresponding to the iron content of 0.07% [36]. In all calculations, molecular weights of 652, 1861 and 42500 were used for hemin chloride, MP-11 and HRP, respectively [31,43].

2.2.3. Kinetic analysis

Kinetic studies on the catalytic oxidation of ABTS and guaiacol (as the known substrates of peroxidase) in the presence of hydrogen peroxide were followed via absorbance changes and electronic spectra using a Varian spectrophotometer model Cary 50 equipped with fiber optic dip probe accessory and xenon light source. The fiber optic probe provides the data recording at the time of mixing in the reaction vessel hence with this probe, no cuvette is required. The ionic strength and pH of the solutions were kept constant by using a 5.0 mM phosphate buffer. Temperature of the reaction solution in the jacketed laboratory reactor (10 mL) was adjusted to 25 °C (±0.1) using a Lauda oil circulating thermobath equipped with an external temperature sensor. Specific activities of the biocatalysts based on ABTS assay were determined spectrophotometrically in a 1-min reaction time course [44]. The specific activity of Fe(III)PPIX-NH_2-FSM16, MP-11-NH_2-FSM16 and HRP-NH_2-FSM16 were obtained 32, 45 and 187 U/mg, respectively. The same spectrophotometer in the kinetic mode was used for recording the progress curves of the oxidation reactions.

2.2.4. Analytical methods

2.2.4.1. Determination of progress of the peroxidative reactions.

2.2.4.1.1. At low concentrations of phenols. Low concentrations of phenolic compound result in formation of dimmers to tetramers, which are soluble in the buffer. In each independent reaction, progress of the product formation was monitored spectrophotometrically at the λ_{max} of the colored product in the 10 mL temperature controlled glass reactor equipped with the fiber optic accessory.

Reactions were carried out in a 10 mL jacketed glass reactor containing 5.0 mL of aqueous sodium phosphate buffer solution (5.0 mM, pH 7.0, 25 °C), specified amount of heterogeneous peroxidase model, about 0.2 mM of aromatic substrate (including: phenol, *ortho*-methoxyphenol (guaiacol), ABTS, phenol/4-aminoantipyrine) and 0.3 mM hydrogen peroxide as the last added reagent.

Progress curve of the each reaction was obtained by following the change in absorbance of the product at its specified λ_{max} values and by obtaining the maximum absorbance change (on the addition of 100 μL of fresh enzyme solution to the reaction mixture at the end of process). The maximum change in absorbance (A_∞) is proportional to the initial amount of the aromatic compound. The percentage of substrate conversion can be determined using the following relations [45]:

$$A_\infty \propto [S]_o; \quad [S]_{consumed} = \left(\frac{A_t}{A_\infty}\right) \times [S]_o \tag{1}$$

$$\%Conversion = \left(\frac{[S]_{consumed}}{[S]_o}\right) \times 100 \tag{2}$$

where A_t and $[S]_{consumed}$ are absorbance and consumed concentration of the aromatic substrate at time t, respectively.

2.2.4.1.2. At high concentrations of phenols. At high concentrations of some phenolic compounds (>0.2 mM) in which a high molecular weight polymer may be obtained, the concentration of remaining phenol at a given time is determined indirectly (at 510 nm) using 4-amino antipyrine reagent [45]. In order to stop the reaction at a specified time 30 μL of 3.0 M sodium azide were added to a 1 mL aliquot from the reaction mixture. After filtering the mixture, the remaining (unreacted) concentration of the phenol was determined in the presence of hydrogen peroxide and fresh concentrated peroxidase (100 μL 0.1%, w/v) by measuring absorbance of the water soluble coloured product (*N*-antipyryl-*p*-benzoquinoneimine) at 510 nm and using a molar absorptivity of (ε_{510} = 7870 cm^{-1} M^{-1}) [45]. The number of moles of the colored product formed is equal to the moles of consumed phenolic compound and then the conversion can be determined according to Eq. (2).

Peroxidatic synthesis of *N*-antipyryl-*p*-benzoquinoneimine from phenol and 4-amino antipyrine were followed spectrophotometrically (at 510 nm) in the presence of hydrogen peroxide using a molar absorptivity of ε_{510} = 7870 cm^{-1} M^{-1} [45]. Peroxidatic synthesis of indophenol from phenol (2.0 mM) and aniline (10.0 mM) was monitored at 630 nm using 3.0 mg MP-11-NH_2-FSM16 and [H_2O_2] = 2.0 mM at pH 7.0, 5.0 mM phosphate buffer solution.

Steady-state kinetics of guaiacol (as a hydrogen donor) and ABTS oxidation by hydrogen peroxide catalyzed by the enzyme model catalysts were obtained [44] in 5.0 mM phosphate buffer, pH 7.0. Progress curves of reactions were obtained at various substrate (ABTS and/or guaiacol) concentrations and the obtained initial rates used to record the Michaelis–Menten curves and obtaining the enzymatic kinetic parameters of the biocatalysts.

In a period of about 30 min during which the progress curves were recorded, specified amounts of catalyst (typically 3.0 mg), guaiacol (0.2–10 mM in the vessel) and hydrogen peroxide (0.3 mM in the vessel) were added, respectively, to a 10 mL temperature controlled vessel and initial rate of reaction (V_o) was calculated from time domain of about 120 s at the linear portion of the curve.

Hydrogen peroxide stock solutions were prepared by appropriate dilutions of 30% (v/v) H_2O_2 in deionized water. Concentration of hydrogen peroxide was determined by absorbance measurements at 240 nm using ε_{240} as 43.6 cm^{-1} M^{-1} [46] and the dilute solutions were freshly prepared. Homogeneous concentrations of MP-11 and HRP were determined at pH 7.0 using molar absorptivities of ε_{395} = 176 mM^{-1} cm^{-1} [47] and ε_{403} = 102 mM^{-1} cm^{-1} [48].

Furthermore, another typical test reaction as the oxidation of ABTS was used for evaluation of capability of the biocatalysts to mimic peroxidase. Progress curves for conversion of ABTS were obtained in the presence of specified amount of the heterogeneous biocatalyst. The amount of Fe(III)PPIX-NH_2-FSM16 was in the range of 1–10 mg, MP-11-NH_2-FSM16 in the range of 0.5–7.0 mg and for the HRP-NH_2-FSM16 was about 0.3–3.0 mg in the reaction mixture of 5.0 mL. Details of experimental conditions are shown in the legends of figures.

Productive synthesis reactions were carried out by means of 2.0 mM of aromatic substrate and excess molar stoichiometric concentration of H_2O_2, which was used by gradual addition by means of a programmable automatic titrator. The reaction mixture was agitated overnight at room temperature and the colored product was then purified by solvent extraction in THF (tetrahydrofurane) and subsequent column chromatography on a 100 cm silica gel column (2 cm diameter).

3. Results and discussion

Fig. 1 shows the XRD pattern of the FSM16 and NH_2-FSM16, which exhibits a strong {1 0 0} reflection peak with one small peak, characteristic of FSM16 mesoporous material [40]. The sample modified with glutaraldehyde (Gl) does not show this characteristic peak, probably because of filling the pore and diminishing the reflectance capability. Interestingly, the enzyme immobilized on this modified mesoporous did not show any peroxidase activity for the aromatic substrate. Hence, it did not use as a support for enzyme immobilization although it showed a high loading of enzyme upon immobilization. The XRD profiles show the low angle sharp peak

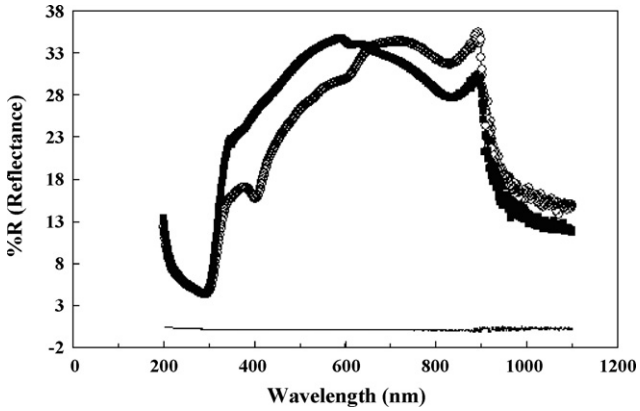

Fig. 2. Solid-state diffuse reflectance UV/Vis electronic spectra for NH_2-FSM16 and MP-11-NH_2-FSM16 samples. (—) Baseline; (■) NH_2-FSM16; (◯) MP-11-NH_2-FSM16.

together with a broad shoulder, characteristics of formation of a disordered hexagonal structure with narrow pore size distribution induced by CTAB surfactant. Hence, specific surface area, pore size distribution and particle size determination were not examined for the samples based on the XRD patterns. Like MCM41, FSM16 consists mostly of long-range ordered hexagonal arrays of uniform mesopores [49,50]. Despite their different synthesis pathways, the pore structures of FSM16 and MCM41 are essentially similar. They have highly uniform, hexagonally arranged, one-dimensional cylindrical pores. The peak at {1 0 0} in X-ray diffractional spectra provides an independent estimate of the pore size in the mesoporous material. Qualitative identification of immobilized amine compound was checked by the ninhydrine test in which generation of a purple colour confirms the existence of amine compound in the FSM sample. Quantitative analysis was done by atomic absorption measurements of the iron content of the samples. Also Fig. 2 shows the diffuse reflectance UV/Vis electronic spectra for the NH_2-FSM16 and MP-11-NH_2-FSM16 catalysts in which the impregnation and substitution of the MP-11 into the mesopores of FSM16 is well characterized at 400 and 650 nm [36,51]. As the figure shows MP-11-NH_2-FSM16 indicates a similar Soret absorption band at 403 nm, very similar to that of the homogeneous peroxidase enzyme.

3.1. Chemical catalysis

Fig. 3 shows typical progress curves for the oxidation of ABTS and guaiacol (in the presence of H_2O_2) catalyzed by the MP-11-NH_2-FSM16 as the peroxidase heterogeneous model catalyst. Theses two reactions are the two common peroxidase assays. Steady-state kinetics of ABTS and guaiacol oxidation by hydrogen peroxide catalyzed by MP-11-NH_2-FSM16 were carried out at λ_{max} of the coloured products of the reactions at 414 nm [52] and 470 nm [53], respectively, in 5.0 mM phosphate buffer, pH 7.0 (as described in Section 2.2.4). As Fig. 3 shows, the reactions were nearly completed within about 20 min. Initial velocities of the oxidation reactions were calculated as the slopes of the initial linear parts of the two shown progress curves. As the figure shows, the reaction is over within about 30 min. Kinetic mechanism of the peroxidase enzyme reaction is well established [54]. The catalytic cycle involves distribution of the enzyme in forms of HRP (free enzyme), and active species CI (compound I) and CII (compound II) [36]. Instantly, when the aromatic substrate is guaiacol, the coloured product of the reaction (in the presence of hydrogen peroxide) catalyzed by HRP appears at 470 nm. Catalysis of the same reaction by MP-11-NH_2-FSM16 biocatalyst produces the same product at 470 nm, which means the catalyst mimics peroxidase.

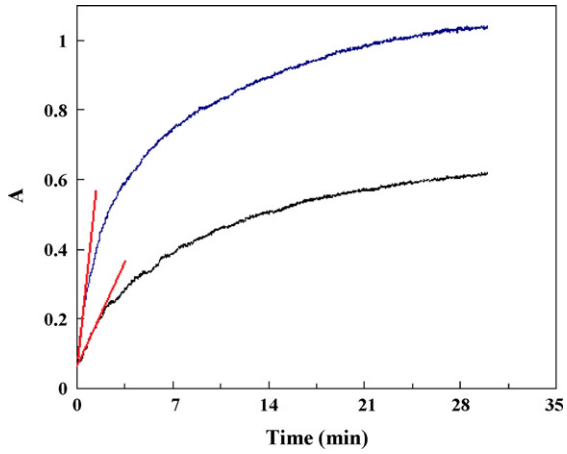

Fig. 3. Typical test reactions for the oxidation of ABTS and guaiacol substrates by the MP-11-NH_2-FSM16 in the presence of hydrogen peroxide, 3.0 mg MP-11-NH_2-FSM16, [ABTS] = 0.2 mM, [guaiacol] = 0.1 mM, [H_2O_2] = 0.3 mM at pH 7.0, phosphate buffer 5.0 mM. Lines shown in the initial part of the progress curves were used for calculation of the initial reaction rates (as slopes of the lines) of the oxidation reactions. Upper (blue), ABTS and lower (black), guaiacol. (For interpretation of the references to color in this figure legend, the reader is referred to the web version of the article.)

In the presence of high concentrations of H_2O_2, an irreversible inactivation process, namely "suicide inactivation process" can also take place for peroxidase ([H_2O_2] > 3.0 mM) [54,55] and microperoxidase-11 ([H_2O_2] > 0.5 mM) [43,56]. To avoid such inactivation effects, experiments were carried out at safe low H_2O_2 concentrations (≤0.3 mM). Using the peroxidase enzyme model, the overall rate of consumption of peroxide can be written as [45,56]:

$$\text{Rate} = \frac{dx}{dt} = \frac{[\text{catalyst}]}{(1/k_1[H_2O_2]_o) + (1/k_3[S]_o)} \quad (3)$$

where S is the reductant (aromatic) substrate. k_1 is the rate constant of the reaction of peroxidase model with hydrogen peroxide resulted in generation of compound I species (a π-radical cation oxoferryl species). k_3 is the rate constant of converting compound II species to the resting state of the hemoenzyme model [36]. Rate constants of k_1 and k_3 can be determined by fitting the experimental data (shown in Fig. 4) into Eq. (3). Common computer software such as Excel Solver was used for this purpose.

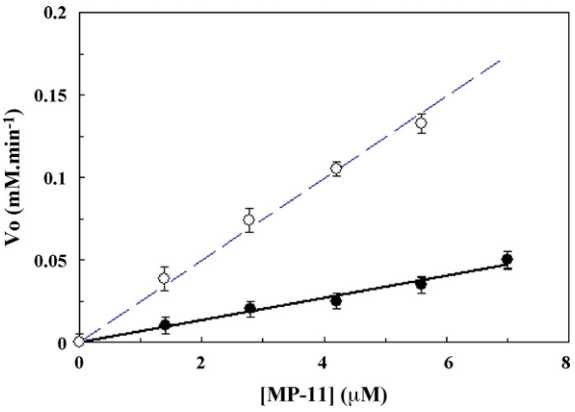

Fig. 4. Initial reaction rates for the oxidation of ABTS and guaiacol substrates as a function of amount of MP-11-NH_2-FSM16 biocatalyst. Reactions were carried out in the presence of hydrogen peroxide 0.3 mM, [ABTS] = 0.2 mM, [guaiacol] = 0.2 mM, [H_2O_2] = 0.3 mM at pH 7.0, phosphate buffer 5.0 mM, using different amounts of the biocatalyst, MP-11-NH_2-FSM16. (◯) ABTS; (●) guaiacol.

Table 1
Comparative rate constants values for HRP and its heterogeneous model catalysts, MP-11-NH_2-FSM16 and Fe(III)PPIX/MCM41

Substrate	MP-11-NH_2-FSM16		Fe(III)PPIX/MCM41[a]		HRP[a]	
	k_1 (s^{-1})	k_3 (s^{-1})	k_1 (s^{-1})	k_3 (s^{-1})	k_1 (s^{-1})	k_3 (sec^{-1})
ABTS	$1.034 \times 10^4 \pm 1.86 \times 10^2$	$1.738 \times 10^3 \pm 26.03$	–	–	–	–
Guaiacol	$3.731 \times 10^4 \pm 5.97 \times 10^2$	$7.540 \times 10^3 \pm 1.38 \times 10^2$	$9.595 \times 10^2 \pm 25$	$1.029 \times 10^2 \pm 3.21$	$1.42 \times 10^7 \pm 2 \times 10^5$	$1.30 \times 10^5 \pm 2.6 \times 10^3$

Rate constants were obtained from fitting of the experimental data into Eq. (3) using Excel Solver as described in Section 3.1.
[a] Values directly taken from ref. [36].

Table 2
Enzymatic kinetic parameters of MP-11-NH_2-FSM16 as the heterogeneous peroxidase model catalyst

	K_m (mM)	V_{max} (mM min^{-1})	k_{cat} (mol S/mol MP-11 s)	Catalytic efficiency (M^{-1} min^{-1})
ABTS	55.8	0.3788	6313.33	1.130×10^8
Guaiacol	55.1	0.3835	6391.66	1.160×10^8
Mean ± S.D.	55.45 ± 1.29	0.3811 ± 0.02363	6352.50 ± 158.81	$(1.145 \pm 0.0297) \times 10^8$

Kinetic parameters were obtained from linear regression of the data of Fig. 5B using Eq. (4) as described in Section 3.2. Turnover number: $k_{cat} = V_{max}/[catalyst]$; catalytic efficiency = k_{cat}/K_m; S: ABTS or guaiacol.

3.2. Peroxidase mimics

Fig. 4 shows variation of initial rates of oxidation reactions of ABTS and guaiacol as a function of amount of biocatalyst. Table 1 indicates the obtained values of the kinetic rate constants for peroxidase activity of MP-11-NH_2-FSM16. Comparison of these k values with those of HRP and Fe(III)PPIX]/MCM41, illustrates the reasonable catalytic activity of the enzyme model catalyst MP-11-NH_2-FSM16 (see Table 1). The method used for calculation of K_m and the other catalytic parameters are described below.

Progress curves and initial rates of the reactions were obtained at various guaiacol and/or ABTS concentrations and were used to sketch the Michaelis–Menten curves as shown in Fig. 5A (inset). Peroxidase enzyme has a K_m value of about 1.5 μM for oxidation of phenolic compounds, such as guaiacol or ABTS [57]. The relevant V_{max} and Michaelis constant (K_m) values for this enzyme model can be obtained from the linear relations of Lineweaver–Burk ($1/V$ vs. 1/[substrate]) and or Eadie–Hofstee models as shown in Fig. 5A and B [58]. Lineweaver–Burk plot includes some restrictions for a reliable estimation of V_{max} and K_m values [36,58], hence analysis based on the Eadie–Hofstee model (Eq. (4)) is preferred, although a close match was observed for Lineweaver–Burk and Eadie–Hofstee plots for MP-11-NH_2-FSM16 biocatalyst upon peroxidatic oxidation of ABTS and/or guaiacol (see Fig. 5A and B):

$$V = -K_m \times \left(\frac{V}{[S]}\right) + V_{max} \quad (4)$$

Previously, values of $K_m = 183.1$ μM and $V_{max} = 0.171$ mM s^{-1} have been obtained for Fe(III)PPIX/MCM41 peroxidase model (encapsulated Fe(III)PPIX into MCM41 mesopores) [36]. Indeed, pore structures of FSM16 and MCM41 (average pore size 3.7 nm) are similar while the pores size of FSM16 can be enlarged up to 6 nm by using a pore expander like triethylbenzene. The obtained K_m and V_{max} values for the MP-11-NH_2-FSM16 model shows a good improvement on preparation of more robust peroxidase biocatalyst and represents high potential for usage of MP-11-NH_2-FSM16 as peroxidase alternative in clinical and biotechnological purposes. Some citable processes include phenol removal from aqueous solutions, oxidation/polymerization of aromatic hydrogen donors (preparation of conductive polymers), epoxidation of alkenes and oxidative coupling reactions in aqueous and organic media. It must be mentioned that there are various limitations for using peroxidase in such industrial processes.

Turnover number or catalytic rate constant (k_{cat}) which represents the maximum number of moles of substrate converted to the product per number of moles of catalyst per unit time,

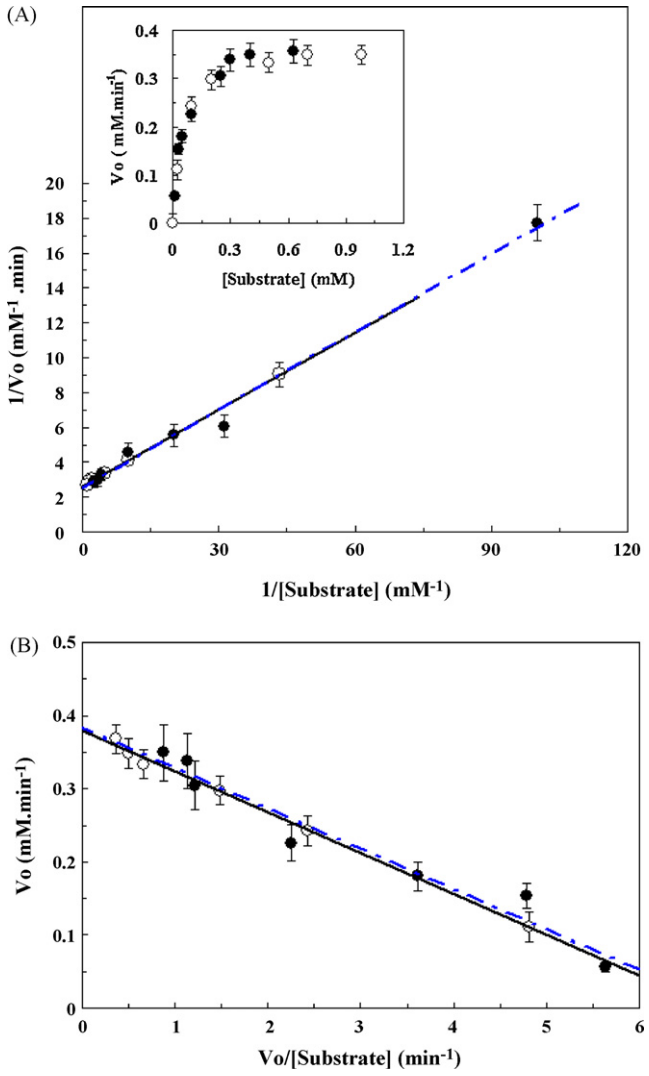

Fig. 5. (A) Lineweaver–Burk plot for the enzymatic behaviour of the heterogeneous peroxidase model, MP-11-NH_2-FSM16 upon oxidation of ABTS and guaiacol. (Inset) The corresponding Michaelis–Menten plot. (B) The corresponding Eadie–Hofstee plot used for estimation of K_m and V_{max} parameters based on Eq. (4). (○) ABTS; (●) guaiacol.

Table 3
Peroxidatic activities of the prepared heterogeneous model enzymes for various oxidation reactions

Heterogeneous model enzyme	Initial reaction rate (mM min^{-1}/mmol biocatalyst)				
	Indophenol synthesis	*N*-antipyryl-*p*-benzoquinoneimine synthesis	Guaiacol oxidation	Phenol oxidation	ABTS: 2,2′-azinobis (3-ethylbenzthiazoline-6-sulfonic acid
Fe(III)PPIX/MCM41	1.0	1.5	2.0	1.4	3.7
Fe(III)PPIX-NH_2-FSM16	1.8	2.3	2.6	1.9	5.3
MP-11-NH_2-FSM16	7.8	12.2	15.5	9.5	23.8
HRP-NH_2-FSM16	1034.7	1308.6	1895.4	1167.3	2165.2

The studied peroxidative reactions are shown in Table 4.

could be obtained as $k_{cat} = V_{max}/[biocatalyst]$. The values K_m, V_{max}, and turnover numbers, k_{cat} (obtained from data of Fig. 5B) were shown in Table 2. Also catalytic efficiencies of the synthetic model enzyme catalyst, which is defined as k_{cat}/K_m were calculated and shown in Table 2. A value of 9.3443×10^4 has been previously reported for the catalytic efficiency of Fe(III)PPIX/MCM41 upon oxidation reaction of guaiacol in the presence of hydrogen peroxide [36]. As it can been seen from Table 2, the value of catalytic efficiency for of MP-11-NH_2-FSM16 is about 10^3 times greater than the value for Fe(III)PPIX/MCM41. This catalytic efficiency is about 100 times lower than the value obtained for homogeneous HRP, $1.67 \times 10^{10}\ M^{-1}\ min^{-1}$ ($k_{cat}/K_m = 2.52 \times 10^4/1.5 \times 10^{-6}$).

Comparison of k_1 and k_3 for MP-11-NH_2-FSM16, Fe(III)PPIX/MCM41 and HRP (see Table 1) shows some meaningful improvement on preparation of more active heterogeneous peroxidase biocatalyst and represents high differences between their catalytic activities. In the case of homogeneous HRP high catalytic activity arises from its naturally engineered structure and high specificity of the enzyme for such substrates and reactions. However, rate constants for the enzyme model catalyst MP-11-NH_2-FSM16 are sufficiently large to complete such reactions in longer periods of time. Peroxidatic activities of the prepared heterogeneous model enzymes for various oxidation reactions are compared and shown in Table 3. Clearly, MP-11-NH_2-FSM16 mimics peroxidase and shows a good catalytic activity upon the peroxidative conversion of substrates, such as typical reactions shown in Table 4.

Although this family of biocatalysts shows good potential for biotechnological purposes but still some important aspects such as designing higher effective and energy-saving reactors and operation under biphasic conditions [59] should also be taken into account in the development of heterogeneous enzyme model catalysts. In addition, there are several limitations for the use of peroxidase in severe industrial conditions. Generally, enzyme structure denatures at high temperatures and pressures, in highly acidic or alkaline media, organic solvents and in the presence of

Table 4
Peroxidative reactions catalyzed by the heterogeneous peroxidase models

Indophenol synthesis	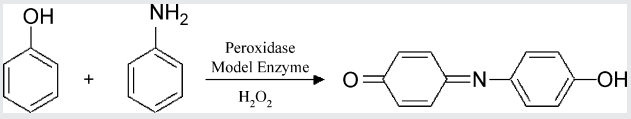
N-antipyryl-*p*-benzoquinoneimine synthesis	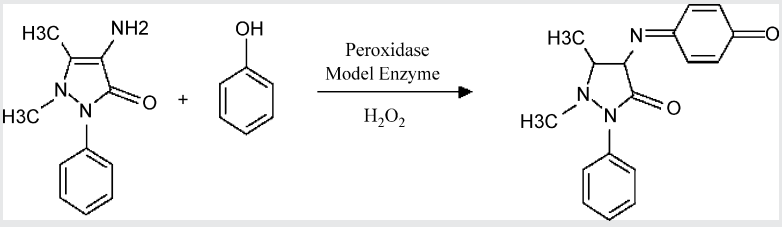
Guaiacol oxidation	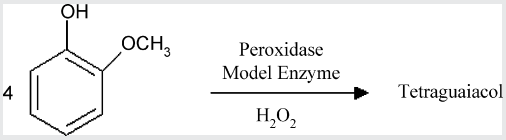
Phenol oxidation	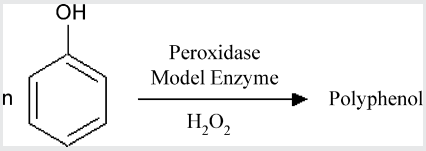
ABTS oxidation	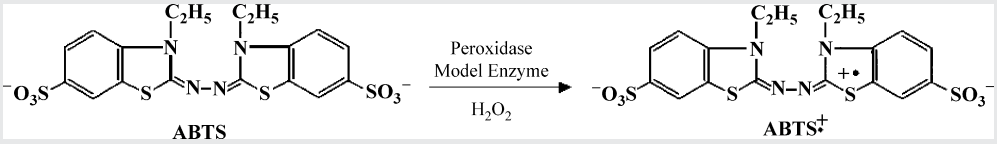

Reactions were carried out at 27 °C, in phosphate buffer 5.0 mM, pH 7.0. The procedure for monitoring the reaction and calculating the reactions rates are described in Sections 2.2.3 and 2.2.4.

denaturants. In most cases, such a denaturation is associated with deactivation of the enzyme. Considering these limitations, inorganic heterogeneous peroxidase models could be introduced as suitable candidates for biotechnological purposes.

4. Conclusion

The advantages of using mesoporous nanostructured-solids as potent enzyme supports have been widely demonstrated however, research on scaling up the reactions and their industrial application in biotechnology and biocatalysis as tailored immobilized homogeneous biocatalysts still seeking much more development. Homogeneous model compounds, peroxidase and miniperoxidase biocatalysts immobilized on mesoporous materials led to generation of heterogeneous peroxidase models with high catalytic activity and efficiency upon peroxidase mimics. Furthermore, they can be potentially used for the catalytic reactions with high specificity in the biotransformation and organic synthesis, biotechnological, environmental, pharmaceutical and agrochemical industries. The use of these heterogeneous peroxidase models in phenol removal from aqueous solutions in a small-size pilot scale (10 L) using a continuous flow glass reactor is the future study in our laboratory.

Acknowledgements

The financial supports of the Research Institute of Petroleum Industry, Iran National Science Foundation and University of Tehran are gratefully acknowledged.

References

[1] R.L. Burwell, Chem. Rev. 57 (1952) 1034.
[2] R.A. Sheldon, Chirotechnology: Industrial Synthesis of Optically Active Compounds, Marcel Dekker, New York, USA, 1993.
[3] J.M. Thomas, R. Raja, Annu. Rev. Mater. Res. 35 (2005) 315.
[4] W. Tischer, F. Wedekind, Top. Curr. Chem. 200 (1999) 95.
[5] P.S.J. Cheetham, in: A.J.J. Straathof, P. Adlercreutz (Eds.), Applied Biocatalysis, Harwood Academic, Amsterdam, The Netherlands, 1999, p. 93.
[6] E. Katchalski-Katzir, D.M. Kraemer, J. Mol. Catal. B 10 (2000) 157.
[7] P. Gemeiner, Enzyme Engineering Immobilized Biosystems, Ellis Harwood, London, UK, 1992.
[8] T. Yanagisawa, Bull. Chem. Soc. Jpn. 63 (1990) 988.
[9] C.T. Kresge, Nature 359 (1992) 710.
[10] D. Zhao, J. Am. Chem. Soc. 120 (1998) 6024.
[11] J.M. Thomas, Angew. Chem. Int. Ed. 44 (2005) 6456.
[12] F. Schuth, Annu. Rev. Mater. Res. 35 (2005) 209.
[13] M. Hartmann, Chem. Mater. 17 (2005) 4577.
[14] H.H.P. Yiu, P.A. Wright, J. Mater. Chem. 15 (2005) 3690.
[15] H.H.P. Yiu, P.A. Wright, in: G.Q. Lu, X.S. Zhao (Eds.), Nanoporous Materials: Science and Engineering, Imperial College Press, London, UK, 2004, p. 849.
[16] X.S. Zhao, Chem. Commun. (1999) 1391.
[17] X.S. Zhao, in: G.Q. Lu, X.S. Zhao (Eds.), Nanoporous Materials: Science and Engineering, Imperial College Press, London, UK, 2004, p. 393.
[18] J.M. Thomas, Acc. Chem. Res. 36 (2003) 20.
[19] X.S. Zhao, X.Y. Bao, W. Guo, F.Y. Lee, Mater. Today 9 (3) (2006) 32–39.
[20] X.S. Zhao, J. Mol. Catal. 191 (2003) 67.
[21] A.S. Maria Chong, X.S. Zhao, Catal. Today 93–95 (2004) 293–299.
[22] H.P.H. Yiu, P.A. Wright, N.P. Botting, Microporous Mesoporous Mater. 44/45 (2001) 763–768.
[23] H. Takahashi, B. Li, T. Sasaki, C. Miyazaki, T. Kajino, S. Inagaki, Microporous Mesoporous Mater. 44/45 (2001) 755–762.
[24] B.F.G. Johnson, Chem. Commun. (1999) 1167.
[25] S.A. Raynor, Chem. Commun. (2000) 1925.
[26] P. Wang, Biotechnol. Bioeng. 74 (2001) 249.
[27] M. Tortajada, J. Mater. Chem. 15 (2005) 3859.
[28] H. Hatzikonstantinou, S.B. Brown, Biochem. J. 174 (1978) 893–900.
[29] P. Jones, D. Mantle, I. Wilson, J. Chem. Soc., Dalton Trans. (1983) 161–164.
[30] P. Jones, T. Bobson, S.B. Brown, Biochem. J. 135 (1973) 353–359.
[31] R.W. Hay, Bio-Inorganic Chemistry, Ellis Harwood Limited, New York, 1991.
[32] G. Palmer, in: D. Dolphin (Ed.), The Porphyrins, Academic Press, New York, 1978.
[33] D. Portsmouth, E.A. Beal, Eur. J. Biochem. 19 (1971) 479–487.
[34] N. Kamiya, M. Goto, S. Furusaki, Biotechnol. Bioeng. 64 (4) (1999) 502–506.
[35] X.S. Zhao, G.Q. Lu, G.J. Millar, Ind. Eng. Chem. Res. (1996) 2075–2090.
[36] K. Nazari, S. Shokrollahzadeh, A. Mahmoudi, F. Mesbahi, N. Seyed-Matin, A.A. Moosavi-Movahedi, J. Mol. Catal. A 239 (2005) 1–9.
[37] A.S.M. Chong, X.S. Zhao, Catal. Today 93 (2004) 293.
[38] H. Takahashi, B. Li, T. Sasaki, C. Miyazaki, T. Kajino, S. Inagaki, Microporous Mater. 44/45 (2001) 755–762.
[39] X.S. Zhao, G.Q. Lu, G.J. Millar, X.S. Li, Catal. Lett. 38 (1996) 33–36.
[40] S. Inagaki, Y. Fukushima, K. Kuroda, J. Chem. Soc. Chem. Commun. (1993) 680–682.
[41] S. Inagaki, A. Koiwai, N. Suzuki, Y. Fukushima, K. Kuroda, Bull. Chem. Soc. Jpn. 69 (1996) 1449.
[42] A. Taguchi, F. Schuth, Microporous Mesoporous Mater. 77 (2005) 1–45.
[43] M. Khosraneh, A. Mahmoudi, H. Rahimi, K. Nazari, A.A. Moosavi-Movahedi, J. Enz. Inhib. Med. Chem. 22 (6) (2007) 677–684.
[44] K. Nazari, A. Mahmoudi, M. Khosraneh, Z. Haghighian, A.A. Moosavi-Movahedi, J. Mol. Catal. B (2008), doi:10.1016/j.molcatb.2008.04.008.
[45] K. Nazari, N. Esmaeili, A. Mahmoudi, H. Rahimi, A.A. Moosavi-Movahedi, Enz. Microb. Technol. 41 (2007) 226–233.
[46] P. George, Biochem. J. 54 (1953) 267–271.
[47] M. Oyadomari, M. Kabuto, H. Wariishi, H. Tanaka, Biochem. Eng. J. 15 (2003) 159–164.
[48] A.X. Maehly, B. Chance, in: S.P. Colowick, N.O. Kaplan (Eds.), Methods Enzymology, vol. 2, Academic Press, New York, 1965, pp. 764–775.
[49] C.Y. Chen, H.X. Li, M.E. Davis, Microporous Mater. 2 (1993) 17–26.
[50] H.Y. Zhu, X.S. Zhao, G.Q. Lu, D.D. Do, Langmuir 12 (1996) 6513–6517.
[51] B.T. Holland, Ch. Walkup, A. Stein, J. Phys. Chem. B 102 (1998) 4301–4309.
[52] R.E.C. Bardsley, G. William, Biochem. J. 145 (1975) 93–103.
[53] A.C. Maehly, B. Chance, in: S.P. Colowick, N.O. Kaplan (Eds.), Methods Enzymology, vol. 2, Academic Press, New York, 1965, pp. 764–775.
[54] K.J. Baynton, J.K. Bewtra, N. Biswas, K.E. Taylor, Biochim. Biophys. Acta 1206 (1993) 272–278.
[55] A.N.P. Hiner, J. Hernandez-Ruiz, M.B. Arnao, F. Garcia-Canovas, M. Acosta, Biotechnol. Bioeng. 50 (1996) 655–662.
[56] A.C. Maehly, Methods Enzymol. 2 (1972) 801–813.
[57] N. Kumar, D.R. Tripathi, Plant Peroxidase Newslett. 15 (1999) 45–48.
[58] T. Palmer, Understanding Enzymes, 3rd ed., Ellis Harwood Publication, Sussex, 1991, pp. 118–125.
[59] D.J. Cole-Hamilton, Science 299 (2003) 1702.